



Multilevel Features Fusion of Intelligent Techniques for Brain Imaging Analysis

Talib A. Al-Sharify¹, Mohammed Hussein Ali², Aqeel Hussien³, Zaid Saad Madhi⁴

¹ Computer Communication Department, Al Rafidain University College, Baghdad, Iraq

² Department of computer engineering techniques, Mazaya University college, Thi Qar, Iraq

³ Department of medical instrument engineering techniques, Alfarahidi University, Baghdad, Iraq

⁴ Radiological Techniques Department, Al- Mustaqbal University College, 51001 Hilla, Iraq

Emails: Talib.abdzaid.elc@ruc.edu.iq ; Mohammed.hussein@mpu.edu.iq ; Aqeel.hussen@alfarahidiuc.edu.iq ; zaid.saad@uomus.edu.iq.

Abstract

With the use of multi-level features fusion, this work provides a new method for recognizing cognitive brain activity, which we term the Improved Multi-modal cognitive brain-imaging method (IMCBI). Identifying brain areas and basing judgments on insights into intelligent cognitive behavior for babies and adolescents presents a number of methodological issues that the suggested approach seeks to address. In order to understand how the brain functions during various motor, perceptual, and cognitive tasks, IMCBI employs smart methods for fusing data at several levels. This technique employs functional magnetic resonance imaging (fMRI) data to assess human behavioral activity in the brain while engaging in a variety of activities. It does so by combining an inter-subject retrieval strategy with deep neural networks (DNN). The research shows that the suggested method, which uses multi-level fusion of features, greatly raises the accuracy ratio to 95.63 percent, the sensitivity to 95.42 percent, and the specificity to 94.3 three point three percent. The findings demonstrate the method's efficacy in recognizing brain activity based on high-level cognitive ability, making it a useful tool for predicting clinical and behavioral responses.

Keywords: Cognitive intelligence; Multilevel Fusion brain imaging; Neuroimaging model; function MRI; brain activity recognition.

1. Introduction

The development of the brain undertakes functional and structural transformation throughout its lifetime[1]. The advancement, cognitive change of mind, and the correlation among neurocognitive improvement are less established throughout children and teens[2]. Experiments that explain how the training and learning map of structural, connective, and physiological changes in the cerebrum through children and adolescents are focused[3]. Modern non - destructive brain imaging techniques have allowed researchers to observe the brain's cognitive development and functions securely[4]. The cognitive neuroscience approaches have been developed by explaining morphological and chemical structure improvements in brain development. Such tests include an approximate assessment of brain structure and function[5]. Collaboratively, the knowledge of average brain growth and neurobiology strengthens the understanding of adverse psychological mechanisms through sophisticated MRI technologies such as diffusion-weighted pictures and fMRI[6]. Combined with data from the electroencephalogram (EEG), these interventions include a profound summary of the functional and psychological variations of autism spectrum disorder (ASD) and communication representation problems[7]. Cross-section scans with brain science techniques reveal, in particular, that the neural fundamentals of developmental symptoms do not include knowledge sharing through dispersed brain regions; they have important properties in the central cerebellum.

Recent empirical MRI findings have presented the most convincing evidence of behavior change during early adolescence with growth. [8] Firstly, the main essential areas, for example, motor and cognitive systems, are

advanced early with time and cerebellum organizations linked with language components and messages reaching maturity in spaces. [9] These data are compatible with autopsy studies on non-human and human primates that demonstrate that the cortex develops in ultimate capacity at rates more extended than the brain's cortex. [10] A cross-sectional brain secretion study among infants and teenagers showed similar trends that throughout the time, white matter absence represents a sculpture in the correct working adult of the developing brain. [11] Therefore, it is recommended to model the path of behavior continuing socially destructive neural activities like replanting and link loss. Nowadays, few studies link brain connectivity to a cognitive evolution, while implicit brain structure measurements indicate economic development and probably the functioning of the frontal lobe. [12] In the growth and development of more extraordinary cognitive ability, the growth of the frontal lobe should be seen as a significant factor. [13] The capacity to scan and remove useless information and behavior for the appropriate ones describes knowledgeable cognitive abilities. [14] In image studies, several anatomical and physiological variations exist among children and young adults. [15] Such variations include height, breath, heart rate, blood pressure, and neural capacity. [16] Indeed, personality disparities should be considered by comparing age classes. For example, kids could have more uncertainty in the experiment than adolescents, affecting their desire and ability to interpret and meet the study's objectives. [17] These variations between teenagers and adults are usually larger and can vary based on gender and maturity. [18] The activity can be more challenging for kids or an interdisciplinary option to achieve these objectives. fMRI offers a convenient, safe way to explore brain formations, which are very important for cognitive skills required for mental data collection and review. A complicated process that occurs over childhood, adolescence, and early adulthood is a good health life cycle in the human nervous system. Brain growth includes complex socialist and regressive procedures that take place in such processes continuously. An application area system can form the human brain, which precisely arranges millions of neurons into modules or operational departments. Recently, brain imaging has developed significant advancements to characterize brain development. Although many behavioral programs are mainly not observed by human beings, they are aware of revealing the basic features of biological brain structure and enhancing understanding of the metabolic operations of the brain as well as the functioning of the brain system. This progress further helped to clarify the dynamic processes of maturation, which led to the emergence of complex cognitive intelligent skills in both atypical and typical aspects.

This work proposes a method to identify brain activity originating from multiple motor, perceptual, and cognitive tasks: the improved multi-modal cognitive brain-imaging approach (IMCBI). The main goal of the proposed strategy is to predict a clinical or behavioral response using brain imaging data. The key contributions are:

- The Improved Multi-modal cognitive brain-imaging technique (IMCBI) proposes a new method for detecting cognitive brain activity by multi-level features fusion
- Intelligent cognitive behavior in newborns and adolescents: overcoming methodological hurdles in region identification and decision making.
- Cognitive, motor, and perceptual processes may all be fused into a single picture using multi-level data fusion approaches.
- Using functional magnetic resonance imaging (fMRI) data, deep neural networks (DNN) are combined with an inter-subject retrieval technique to assess human brain activity while the subject is engaged in a variety of activities.
- It is shown that the suggested method, which uses multi-level features fusion, greatly improves the accuracy ratio, reaching 95.63 percent, the sensitivity, 95.42 percent, and the specificity, 94.33 percent. The Improved Multi-modal cognitive brain-imaging technique (IMCBI) proposes a new strategy for detecting cognitive brain activity by fusing information from many sources.
- Intelligent cognitive behavior in newborns and adolescents: overcoming methodological hurdles in region identification and decision making. Cognitive, motor, and perceptual processes may all be fused into a single picture using multi-level data fusion approaches.
- Using functional magnetic resonance imaging (fMRI) data, deep neural networks (DNN) are combined with an inter-subject retrieval technique to assess human brain activity while the subject is engaged in a variety of activities.
- It is shown that the suggested method, which uses multi-level features fusion, greatly improves the accuracy ratio, reaching 95.63 percent, the sensitivity, 95.42 percent, and the specificity, 94.33 percent.

2. Related Works

Qi Zhu et al. [19] developed Multi-Region Correlation Based Functional Brain Network (MC-FBN). MC-FBN is a method of constructing an efficient distance-based directed brain network. The significant distance can precisely detect the secret distribution of pertinence between all the brain structures to provide a spatial

operating system that continuously represents the knowledge-dispersed paths between active brain regions. The structural information is defined by calculating the two areas' directional possibility and communication intensity. The proposed methods of functional brain systems are more versatile than traditional unguided networks in identifying the operational processes of the brain.

Robert G. Shulman et al. [20] developed A Non-cognitive Behavioral Model (NBM). It directly links reported people's activity to quantified cognitive ability without suggesting intervention in cognitive skills. NBM is based on behavioral science, which expands to provide brain function and actions. The role of neural plasticity in improving the brain's mechanism for cognitive behavior, rather than inherent cognitive abilities, is further strengthened. The new framework is discussed by which the Standard Cognitive Model links cognitive functions to fMRI images and compares them with the NBM. Non-Invasive Imaging Modalities were developed by Ramesh Naidu Annavarapu et al. [21] to investigate illnesses of the aging brain (NIM-DB). With a focus on the core physical ideas of various techniques for non-invasive neuroimaging, the offered methods highlight existing approaches to the visualization of the old mind, which is crucial for neurological study. The invasive neuroimaging techniques employed by cognitive neuroscientists, such as transcranial magnetic stimulation, are described in the first portion of the suggested procedure (TMS). The second section gives a thorough rundown of numerous image technology computational models for various neurological investigations in the aging brain. According to Zhe Wang et al. [22], Cognitive Impairment and Normal Control Subjects Using fMRI-Based Network Connectivity Analysis. (CIN-NCA). With confined fMRI-sized data, the proposed methodology uses functional brain analysis methodologies to identify mild cognitive impairment (MCI), Alzheimer's disease (AD), and Alzheimer's disease (AD). To compare all relevant ROI pairs with function vector, the first section selects an area of interest (ROI) within the traditional wired networks. Second, we provide a regularised Linear Discriminant Analysis (LDA) method to reduce noise and limited sample sizes.

Wei Chun Ung et al. [23] introduced the Novel visual Working memory (VSWM) method. The effects of rising workloads were explored by functional near-infrared spectroscopy (fNIRS) cortical correction via a creative visual working memory (VSWM) form. Due to its importance in VSWM and neural regulation, the bilateral prefrontal cortex (PFC) was investigated. There were 31 healthy controls (HCs), 12 Mild Cognitive Impairment patients, and 18 mild Alzheimers patients (mADs). The results supported the relationship between neural compensation and cognitive load theory. The study results showed that neural compensation could have been induced with the proposed VSWM task Correct mental quantity.

Antonio R. Porras et al. (LAD-SR) use locally affine diffeomorphic surface registration. A suitable procedure plan is created for each patient using a locally affine diffeomorphic surface registration technique. The suggested methodologies estimate the optimal processing schedule by decreasing anomaly in the vertebral type, measured using quantifiable measurements using a standard vertebral model built from a total of 198 safe examples. The sum of each bone component and the translation, rotation, and bending positions are swiftly and efficiently arranged using front-orbital osteotomy models. Wenxing Hu et al. [25] proposed deep collaborative learning (DCL). First, deep collaborative learning uses an in-depth system to reflect and identify similarities between the source information and phenotypic knowledge. To detect the variation of Functional Connectivity observed between different ages, and used Functional Connectivity as fingerprints. The proposed method has shown tremendous success with the DCL in categorizing communities of varying ages and significantly compared with other traditional designs. The results showed that DCL is comparable to standard data fusion. A better brain relationship highlights the importance of the brain development phase in adolescence.

As observed from the literature study, The human brain experiences imperative changes in its structural and functional architecture across its lifespan. Recently, brain imaging has developed significant advancements to characterize brain development. Hence, this paper proposes the Improved Multi-modal cognitive brain-imaging method (IMCBI) to perceive brain activities from different motor, perceptual, and cognitive tasks.

3. Improved Multi-modal cognitive brain-imaging method (IMCBI)

An improved Multi-modal cognitive brain-imaging method (IMCBI) has been proposed to perceive brain activities from different motor, perceptual, and cognitive tasks. The use of mental success-dependent information for actual observations strengthens the Multi-modal cognitive (MC) method training. The inter-subject retrieval method uses deep learning algorithms to interpret behavioral activities in the human brain performing various tasks collected from functional magnetic resonance imaging (fMRI) data. The overall architecture of the Improved Multi-modal cognitive brain-imaging method is shown in figure 1.

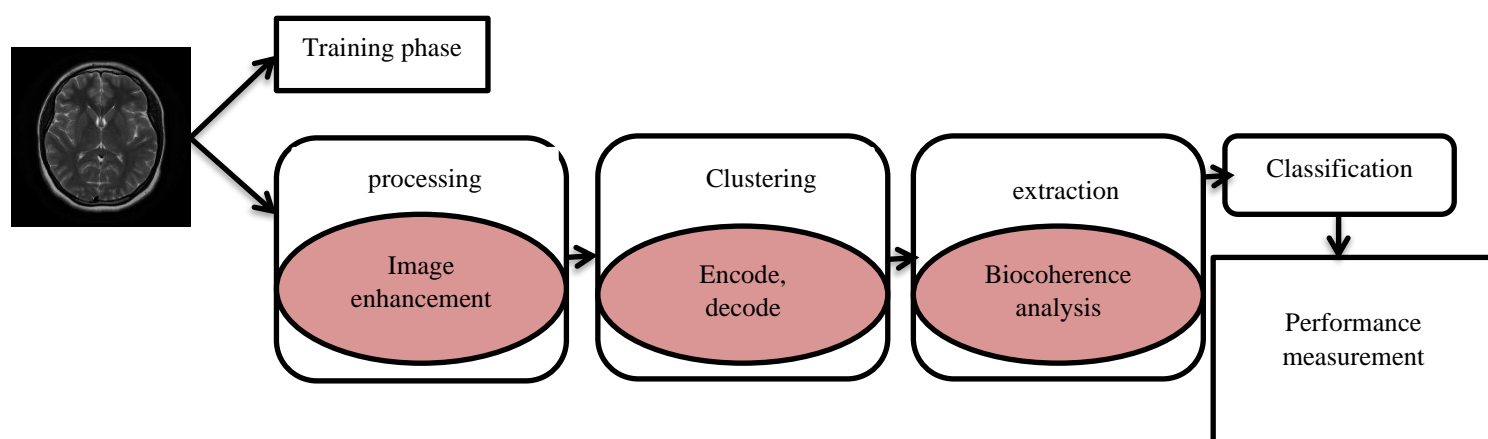


Figure 1: The overall construction of the Improved Multi-modal cognitive brain-imaging method

Improved Multi-modal cognitive brain-imaging method has a training and testing phase. [29]The stages of the brain imaging method involve pre-processing, segmentation, feature extraction, and classification.

3.1. Multi-modal cognitive (MC) method

The multi-modal cognitive (MC) method is based on findings that the function of human participants is close to optimum pattern recognition in many detection techniques. The human vision's neurocognitive feature and the MC's discriminating feature (evaluating the length of a template to the dividing border) indicate that such two parameters match well. The finding suggests a clear correlation between appropriate trend classifiers and human interactions. In the Multi-modal cognitive (MC) method, individual participants are first prepared to complete a visual classification task among two groups of stimuli before achieving steady efficiency. Based on the preparation, the observations conducted a detection system throughout fMRI screening. To everyone's understanding, the Multi-modal cognitive (MC) method requires human spectator intervention to enhance the object training phase. Stimulation is split into two sections in the building phase. The main objective is to construct a model to determine the labeling of stimulus-dependent on the brain cell actions they induce. In the analysis, two types of data sources are collected. The first data is the brain cell operation, which is recalled by triggers, and it is denoted as a_r for $r = 1, 2 \dots X$ and where X is the maximum series of experiments for the known class labeling, which is expressed by $b_r = 1$ or -1 . The individual observatories' neurocognitive ability, which is defined as $x(t_s)$ for each t_s it has a value for $s = 1 \dots Y$. Concerning the categorization task, there is an option to select $S = 6$, six different enhance situations, and interference is applied to create multiple iterations with the same improved conditions. Every other stimulation is applied to a single brain cell structure. With each simulation circumstance, the neurocognitive method tests the classification errors of the individual observatory. In general, a similar trend to the dividing line, the better the likelihood of mistaken identification of human searching. The neurocognitive feature could provide important information about some system's possible range from the border. The understandings and experiences are the quantitative feature in the field to the limit, and it is explained in equation (1)

$$\left. \begin{aligned} b_r &= |2x(t_s) - 1| \text{ for } a_r \in t_s \ 0 < x(t_s) < 1 \\ b_r &\geq 1 \text{ for } a_r \in t_s \ x(t_s) = 1 \text{ or } x(t_s) = 0 \end{aligned} \right\} \tag{1}$$

As obtained from Equation (1), the first data is the brain cell operation, which is recalled by triggers, and it is denoted as a_r , b_r is the known class labeling, individual observatories neurocognitive ability is denoted as $x(t_s)$. In this case, the situation $a_r \in t_s$ means that the a_r does stimulation produce the sequence t_s . For instance, training a_r , for $r = 1, 2 \dots X$ are separated into two ranges. The quantity of essential instances is denoted as X_1 . The other form is practical training with a longer distance than the limited one. These are the same conditions that human observers do not have a failure in identification, meaning they are very far from the boundary. The matching is done for all instances, and the first value X_1 is enabled for empirical validation. The objective function is symmetric and has an optimal solution, which does not affect learning efficiency. In the detection stage, there is the use of spatial information. The multi-modal cognitive method's discriminatory feature is described as shown in equation (2)

$$g(a) = v.A + d * a_r * x(t_s) + b_r * x(t_s) \tag{2}$$

As obtained from Equation (2) v represents the spatial information, $g(a)$ represents a discriminatory feature, $x(t_s)$ represents the individual observatories' neurocognitive ability. The corresponding cost function d is reduced by optimizing its variables, and it is explained in equations (3) and (4)

$$\min_{v,d,\pi,\varepsilon} \frac{1}{2} \|v\|^2 + \frac{B}{2} \sum_{r=1}^{R_1} \pi_r^2 + \sum_{r=R_1+1}^R \varepsilon_r \tag{3}$$

$$\begin{cases} b_r(v \cdot a_r + d) = c_r - \pi_r \text{ for } 1 \leq r \leq X_1 \\ b_r(v \cdot a_r + d) \geq 1 - \varepsilon_r \text{ for } X_1 \leq r \leq X \\ \varepsilon_r \geq 0 \text{ for } X_1 \leq r \leq X \end{cases} \tag{4}$$

As inferred from Equation (3), the cost function d is reduced by optimizing its variables, v, d, π, ε represents the optimizing variables, b_r as class labeling. The first data is the brain cell operation, which is recalled by triggers, and it is denoted as a_r .

The quantity of essential instances is denoted as X_1 , here the multi-modal cognitive (MC) method has additional equivalent limitations $1 \leq r \leq X_1$ for crucial instances and compared to standard ones. The functionality rate is represented as $\frac{B}{2} \sum_{r=1}^{R_1} \pi_r^2 + \sum_{r=R_1+1}^R \varepsilon_r$. π_r Which is the optimization variable that is not needed because interaction occurs by raising or reducing the gap is an equal chance. The Lagrangian component is achieved as described by following the correct variational procedure as shown in equation (5)

$$L(v, d, \varepsilon, \gamma, \rho) = \frac{1}{2} \|v\|^2 + \frac{B}{2} \sum_{r=1}^{X_1} \pi_r^2 + D \sum_{r=X_1+1}^X \varepsilon_r - \sum_{r=1}^{X_1} \gamma_r [b_r(v \cdot a_r + d) \cdot c_r + \pi_r] \tag{5}$$

As obtained from Equation (5), $L(v, d, \varepsilon, \gamma, \rho)$ represents the Lagrangian component, the functionality rate is defined as $\frac{B}{2} \sum_{r=1}^{X_1} \pi_r^2$. The correct variational procedure is represented by $b_r(v \cdot a_r + d) \cdot c_r$. The variations are between the limitations for γ^r as objective function. Consequently, Multi-modal cognitive prediction is written as shown in equation (6)

$$g(a) = \sum_{\gamma \in TU} a_r b_r \cdot b + d + \frac{B}{2} \sum_{r=1}^{X_1} \pi_r^2 \tag{6}$$

As inferred from Equation (6), b , and d are the implement variables, and those have not vanished that a_r for $R > X_1$. Measurement d is dissimilar from many limitations of equal opportunities for the Multi-modal cognitive (MC) method. The important notice is that the mentioned strategy would work quite well if the number of essential illustrations is large enough, as shown in equation (7)

$$d = \frac{1}{X_1} \sum_{r=1}^{X_1} (v \cdot a_r - b_r \cdot C_r) \tag{7}$$

As obtained from equation (7), here, d is dissimilar from many limitations of equal opportunities for the Multi-modal cognitive (MC) method. The correct variational procedure is denoted as C_r, b_r as class labeling. The first data is the brain cell operation, which is recalled by triggers, and it is denoted as a_r . The labeling of data in the brain image is shown in figure2.

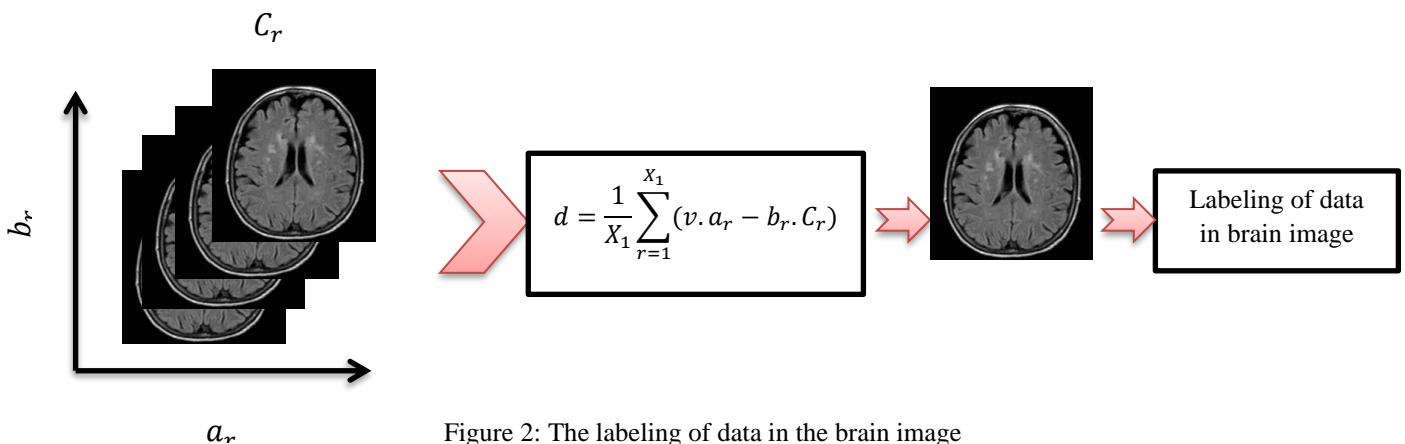


Figure 2: The labeling of data in the brain image

3.2. The inter-subject retrieval method

The inter-subject retrieval (ISR) method makes use of the Deep Neural Network (DNN) to interpret behavioral activities in the human brain performing various tasks that are collected from the functional magnetic resonance imaging (fMRI) data.

a. Data acquisition and pre-processing

The photos from global processing images with different brightness, picture quality, and intensity are found in the Kaggle datasets [26]. Standardization of these characteristics is completed at this stage, which helps to promote the ISR technique by resulting in a higher sensitivity rate[27-29]. As previously noted, pre-processing is done, and the input photos have been modified to a particular direction of the maximum area scale. The image becomes closer once the radius is set to a specific size in the first phase. Equation illustrates a system for lighting equalization and brightness optimization that is utilized to achieve a higher sensitivity rate (8)

$$X_1(a, b; \pi) = \gamma(R(a, b) - g(a, b; \pi) * R(a, b)) + \delta \quad (8)$$

As inferred from the above equation, $g(a, b; \pi)$ is the kernel Gaussian for the blending of the image with standard deviation $R(a, b)$. Constraint δ shows a dissimilarity, and γ preserves the majority of the frequencies of the vectors in the range of [a,b]. Every color image stream R is processed separately in equation (1). By removing spherical boundary shells and covering the sections inside the outside surface of the given area, the X_1 ultimately involves the removal of colorful boundaries. Unwanted picture contrast may be the result of the longitudinal and transverse balance being uneven. Figure 3 depicts the image's pre-processing stage.

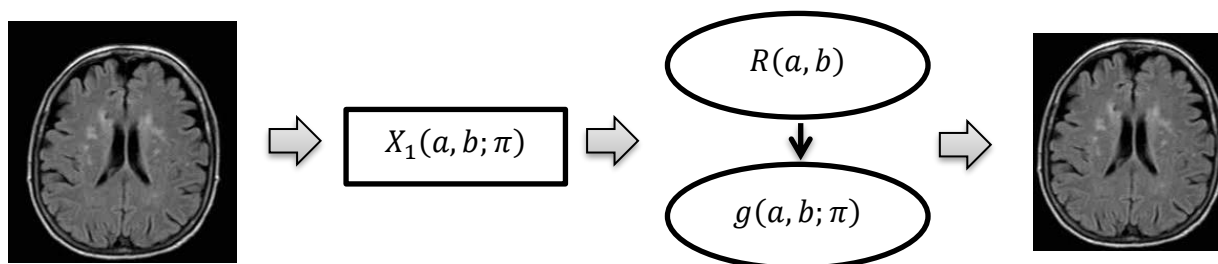


Figure 3: The pre-processing phase of the proposed method

b. Segmentation stage

The receptive space of the linear combination can be modified, and various enlarged proportions are used. Equation (9) states that when the increased ratio is x , the size of the linear interpolation filter is b , and a is a single observation layer with extended matrices.

$$X_r = (a - 1) \times (b - 1) + p * R(a, b) \quad (9)$$

As obtained from Equation (9), for example, using a spatial dimension of 2×2 , an enlarged ratio x is assigned to 3, and the precise, reactive measurement is set to 8. Assembling some observation levels frequently permits a broader field to be obtained accurately.

The diluted activation function is possible to obtain a broader application in the field in comparison with the conventional converting device with no increment shown in equation (10)

$$b[r] = \sum_{x=1}^x a[x + b \times r] \times v[r] \quad (10)$$

As inferred from Equation (10), $a[r]$ input image, $b[r]$ output image, $v[r]$ specific filter of r^{th} factor, r is the length of the filter. The above equation reduces the normalized observation layer to $b=1$ to increase the specificity rate.

1. Encoding stage

The design of the encoder and other segmentation stage elements determines whether an activity or an abnormal brain image may be detected. The fast route technique makes the network model substantially more responsive to weight shift, enabling faster mass adjustments of the convolution layer.

2. Decoding of images

In sensory computation, brain activity was measured and used to analyze things and brain functions in stimulation or cognitive functions. Sensory information is the most remarkable effort in mental images,

including sequencing, sensory perceptions, visual data decryption, and restoration of the visual stimulus. Besides, some investigators used fMRI to decode the psychological state of visual activities like listening, speaking, and working. But few findings in a large area may decipher various cognitive or behavioral duties. One other drawback of mental decoding is that even the decoder learns the mind asserts from the cognitive function of each person. It was rarely recorded if various subjects were used as a similar converter. As for the approaches used in decoder construction, the inter-subject retrieval (ISR) method is the critical data-driven methodology for recognizing distinct brain patterns of behavior using fMRI datasets as machines for training. The inter-subject retrieval (ISR) method learns, however, primarily deep characteristics from fMRI data as it needs the necessary feature space to pick individually as sources.

Moreover, existing approaches often struggle with feature vector selection differences, which limits their use in the decoder via the topics. DNN is used to know more conceptual brain processing functions. The segment of the input image is shown in figure4.

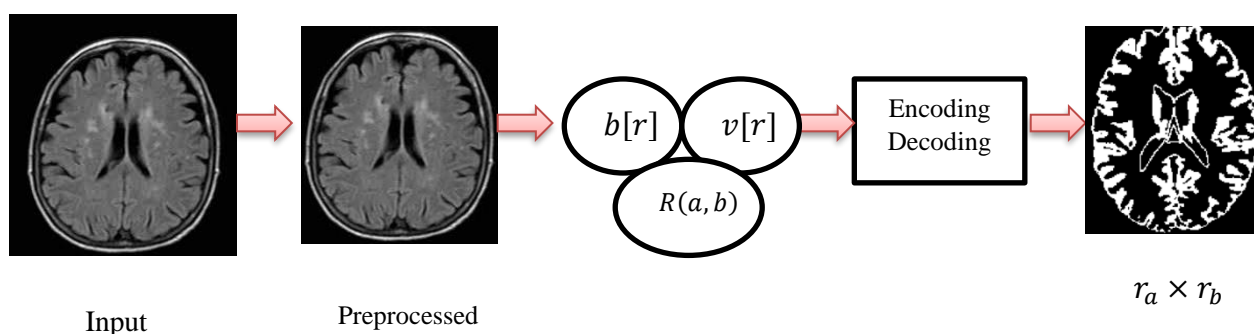


Figure 4: Segmentation stage of the input image

c. Feature extraction

Attributes of a stimulus that can distinguish between the various feelings are analyzed in the feature extraction stage. The EEG data is analyzed by utilizing higher-order wavelengths that are higher-order spatial interpretations or wave cumulative. It is understood that EEG signals are developed by the brain, which would be a device with strongly non-linear parameters, and there is no proof representing the stimulation of the brain. Further, the data is assumed on the EEG signals, such as complex and non-Gaussian data, which should be used. An essential aspect of ISR lies in its ability to detect variational contacts among stages in the higher-order spectral range, and this is referred to as quadratic image acquisition. Features of the higher-order of signal, including the bispectrum, are examined in the proposed method. Bicoherence analyses investigate the connection between two central wavelengths of curved substances g_1 and g_2 , and the wavelength $g_1 + g_2$ propagation element. Specific frequency sections of this category are referred to as three g_1 , g_2 , and $g_1 + g_2$ used to determine the cognitive behavior of infants and adolescents. The bicoherence is the transition from the special relativity of the frequency's higher-order generation system, and it is explained in equation (11)

$$bicoherence(g_1, g_2) = F[Y(g_1).Y(g_2).Y^*(g_1 + g_2)] \tag{11}$$

As inferred from the above equation, Y^* Represents characteristic impedance, $F[]$, is the assumption task. Very few element waves are connected to or linked if a waveform bicoherence is a nil. If the bicoherence of a real signal is not aliased, it is explicitly represented in the triangular form $g_2 > 0, g_1 > g_2, (g_1 + g_2) < \pi$. As a linear function of distinct bicoherence, it consists of particular areas with similarities (g_1, g_2) level for the working mechanism. Most of these areas are evident, as shown in equation (12)

$$\left. \begin{aligned} bicoherence(g_1, g_2) &= bicoherence(g_2, g_1) = bicoherence(-g_1 - g_2, g_2) \\ &= bicoherence(-g_1 - g_2, g_1) = bicoherence(g_1, -g_1 - g_2) \\ &= bicoherence(g_2 - g_2, -g_1) \end{aligned} \right\} \tag{12}$$

As obtained from equation (12), two central wavelengths of curved substances are denoted as g_1 and g_2 , and the level of the working mechanism of the brain is explained in a detailed manner. The standardized bicoherence is established and defined in equation (13)

$$bicoherence(g_1, g_2) = \frac{bicoherence(g_1, g_2)}{\sqrt{Q(g_1).Q(g_2).Q(g_1+g_2)}} \tag{13}$$

As inferred from equation (13), $Q(g)$ is the power range. Standardized bicoherence techniques extract many features from the brain image, is illustrated in figure5

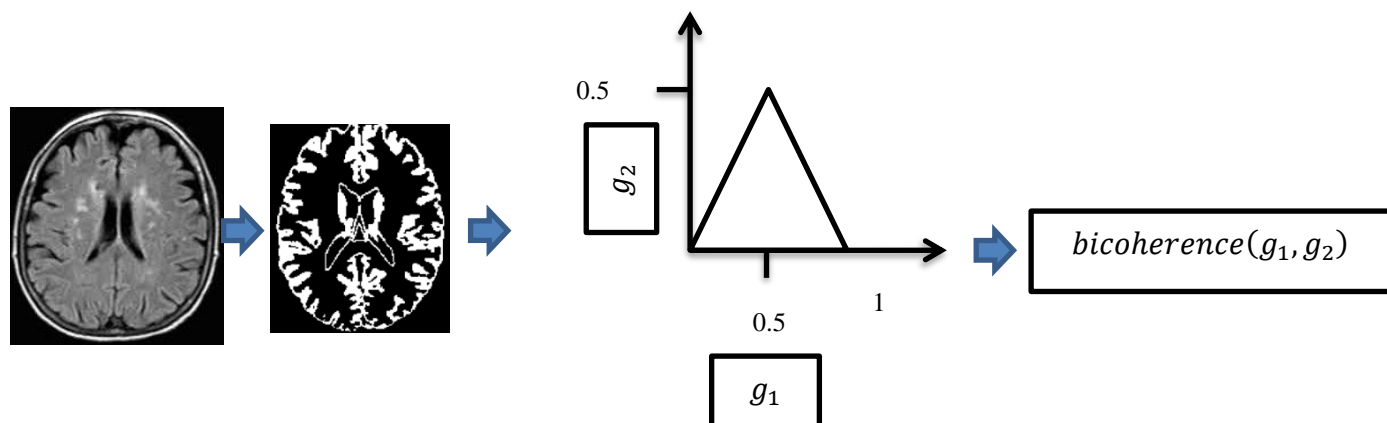


Figure 5: Standardized bicoherence techniques extract many features from the brain image

d. Classification of the image

Data discovery by constructing a vector for identifying the main component is the first step after standardization. Further, if the error of minimum grouping is different, this vector is replaced with input data. If $a_1, a_2 \dots a_R \in T^R$ and $b_1, b_2 \dots b_S \in T^R$ are the information trained for various stages, a_R is the information from the s -th stage, b_S is the information trained from $(s+1)$. The current vector used to locate the linear combination which describes R . $R = a \cup b$, R is denoted as $R = (a_1, a_2 \dots a_R, b_1, b_2 \dots b_S) \in T^R$. The Linear combination of a vector can be represented as $R(D_R)$ and it is explained in equation (14)

$$D_R = \frac{1}{R+S} (\sum_{s=1}^R a_s a_s^V + \sum_{s=1}^S b_s b_s^V) \tag{14}$$

As inferred from the above equation (14) R and S are the linear combinational parameters, D_R is the linear combination vector V is the eigenvector. a_R is the information from the s -th stage, b_S is the information trained from $(s+1)$. The next phase is the optimal solution matrix V and the source vector. Let r be the primary input, u_1 is the nearest comparison matrix that has the very same course to r , and let u_2 is the nearest comparison matrix of category r . The representation for Minimum classification error gives a higher accuracy rate, and it is defined in equation (15)

$$\beta(r) = \frac{l_1(u_1) - l_2(u_2)}{l_1(u_1) + l_2(u_2)} \tag{15}$$

As obtained from equation (15), l_1, l_2 is the gap between Y to u_1, u_2 . If $\beta(r) \in (-1, +1)$, and if $\beta(r)$ image classified properly, else if $\beta(r)$ classified wrongly. $\beta(r)$ decreased for all input data to increase the error rate. The accuracy rate is obtained from the positive values and negative values.

A picture mark of +1 or -1 is given for each image during preparation; +1 denotes the standard brain image, and -1 is the brain image with some activity performance. The linear transfer function is given below

$$R = -(1a = 1) \log(1 - D(r)) + 1(a = -1) \log D(r) \tag{16}$$

As obtained from equation (16), variable predictor are equivalent to 1, 0 if not. Gradient function by DNN shown in equation (17)

$$\frac{\delta R}{\delta D(r)} = \begin{cases} \frac{1}{1-D(r)} & \text{if } \beta(r) = +1 \\ -\frac{1}{D(r)} & \text{if } \beta(r) = -1 \end{cases} \tag{17}$$

As inferred from equation (17), $\frac{\delta R}{\delta D(r)}$ denotes the classification accuracy factor. The linear combination vector D_R . If $\beta(r) \in (-1, +1)$, and if $\beta(r)$ is correct, else if $\beta(r)$ is false.

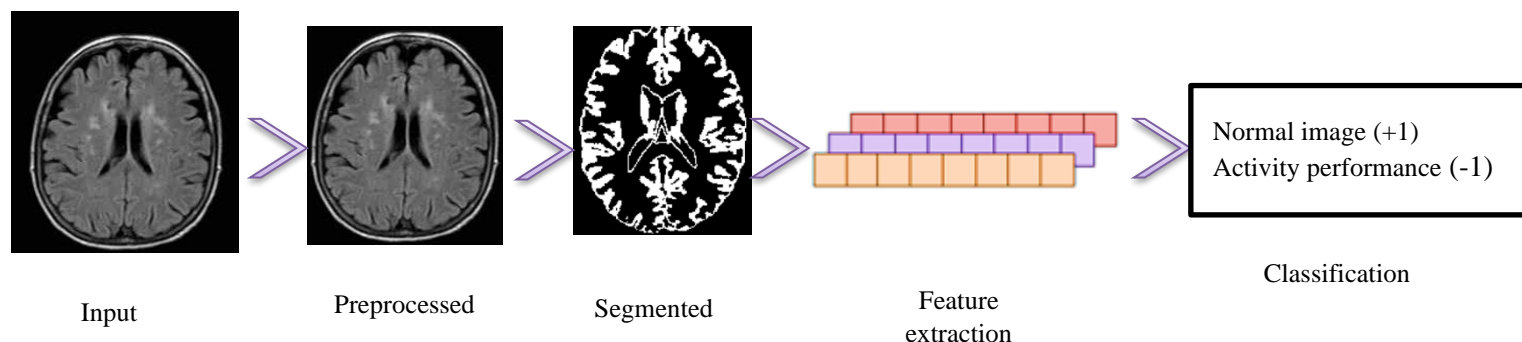


Figure 6: The final stage of classification

{+1, -1} is provided for each image (+1 is for the standard brain image and -1 is for the brain image cognitive behavior for infants and adolescents with some activity performance). The final stage of classification is illustrated in figure6.

In the proposed method, by imperative changes in its structural and functional architecture across its lifespan, advancements are being developed in brain imaging to characterize brain development. This progress further helped to clarify the dynamic processes of maturation, which led to the emergence of complex cognitive intelligent skills in both atypical and typical aspects.

4. Results and discussion

Images from the Kaggle dataset have been used to test the Improved Multi-Modal Cognitive Brain Imaging (IMCBI) approach that has been proposed[26]. Accuracy, Specificity, Sensitivity, and error rate are used to assess IMCBI's performance. Equation (18) describes the proposed method's accuracy.

$$ACCURACY = \frac{t_p+t_n}{t_p+f_p+t_n+f_n} \tag{18}$$

The proposed IMCBI method accuracy is shown in figure7. D_R are represented as the linear combination vector. If $\beta(r) \in (-1, +1)$, and if $\beta(r)$ is correct, else if $\beta(r)$ is false.

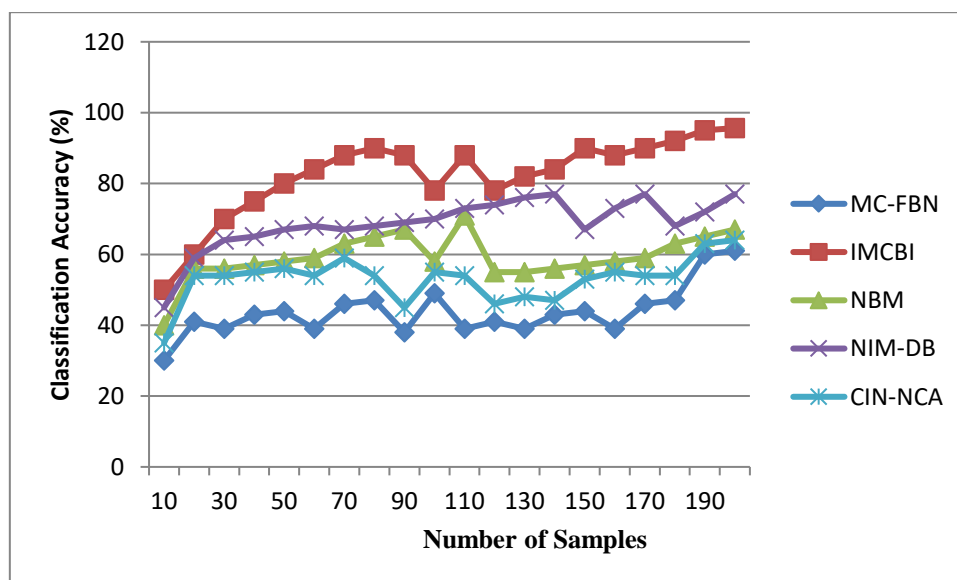


Figure 7: The overall accuracy of the IMCBI method

The sensitivity ratio of IMCBI is defined by Equation (19)

$$Sensitivity = \frac{t_p}{t_p+f_n} \tag{19}$$

Sensitivity is determined by the right positive value and the incorrect negative value, according to equation (19). Based on the established sensitivity ratio, IMCBI is used to detect brain activity on the pictures of the brain. Sensitivity is crucial for detecting brain activity at all stages of classification. Figure 8 displays the suggested IMCBI method's sensitivity rate. IMCBI, or Improved Multi-Modal Cognitive Brain Imaging, is a method for detecting changes in brain activity resulting from various motor, perceptual, and cognitive tasks. The basic objective of the IMCBI approach is to predict a clinical or behavioral response using brain imaging data.

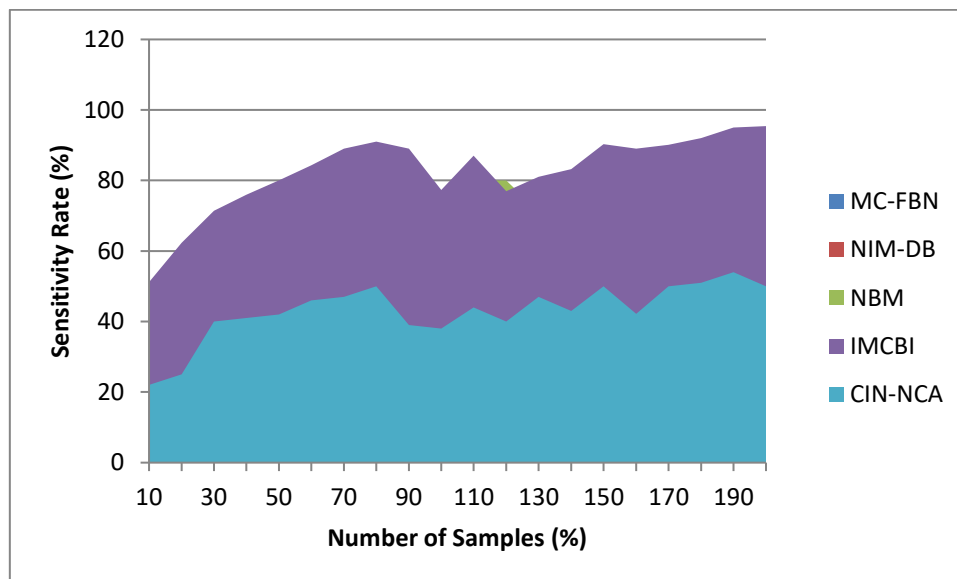


Figure 8: The sensitivity rate of the IMCBI method

Table 1 shows the comparative analysis of the classification accuracy of IMCBI for the training and testing set with sensitivity and specificity. If $\beta(r) \in (-1, +1)$, and if $\beta(r)$ is true, else if $\beta(r)$ is false. $\beta(r)$ is decreased for all input data to increase the error rate. During preparation, a picture mark a $\{+1, -1\}$ is provided for each image (+1 is for the standard brain image, and -1 is for the brain image to perceive brain activities). Further, the probability depends on the directional framework of the classification (the size of a category depends on the same factors and dividing regulations), the most considerable sensitivity and specificity, the smallest deviations, and the most significant possibility.

Table 1: Accuracy, Sensitivity, Specificity of IMCBI

Methods	Training set			Testing set		
	Accuracy	Sensitivity	Specificity	Accuracy	Sensitivity	Specificity
CIN-NCA	85.32	84.23	82.11	84.22	83.11	83.45
NBM	81.23	81.44	80.05	81.67	81.77	81.89
NIM-DB	80.56	80.11	80.27	80.78	80.98	80.34
MC-FBN	79.08	79.89	79.33	79.65	79.55	79.32
IMCBI	95.32	95.11	94.67	95.63	95.42	94.33

The specificity of the proposed Improved Multi-modal cognitive brain-imaging method (IMCBI) is shown in equation (20)

$$specificity = \frac{t_n}{t_n + f_p} \tag{20}$$

The right negative value and incorrect positive value have a significant impact on the specificity rate. The specificity rate categorizes brain images as either a typical, healthy retinal image or an image of diabetic retinopathy. Figure 9 displays the specificity rate of the suggested approach. Brain activity was monitored and employed in sensory computation to assess objects and brain activity during stimulation or cognitive processes.

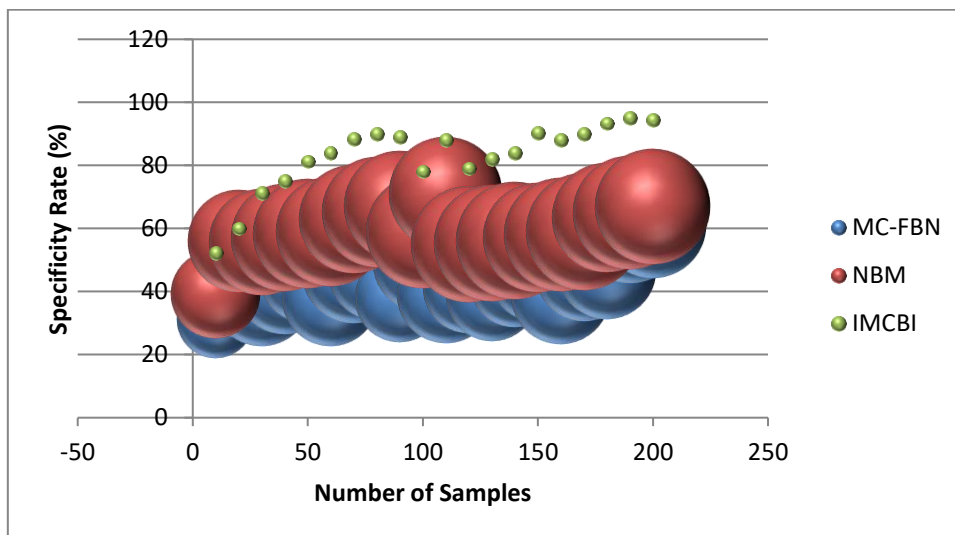


Figure 9: The specificity rate of the IMCBI method

Data discovery by constructing a vector for identifying the main component is the first step after standardization. And if the error of minimum grouping is different, the constructed vector is replaced with input data. The next phase is the optimal solution matrix V and the source vector. Let r be the primary input, u_1 is the nearest comparison matrix that has the very same course as r, and let u_2 as the nearest comparison matrix that has a separate category from r. The representation for the Minimum classification error is shown in figure 10.

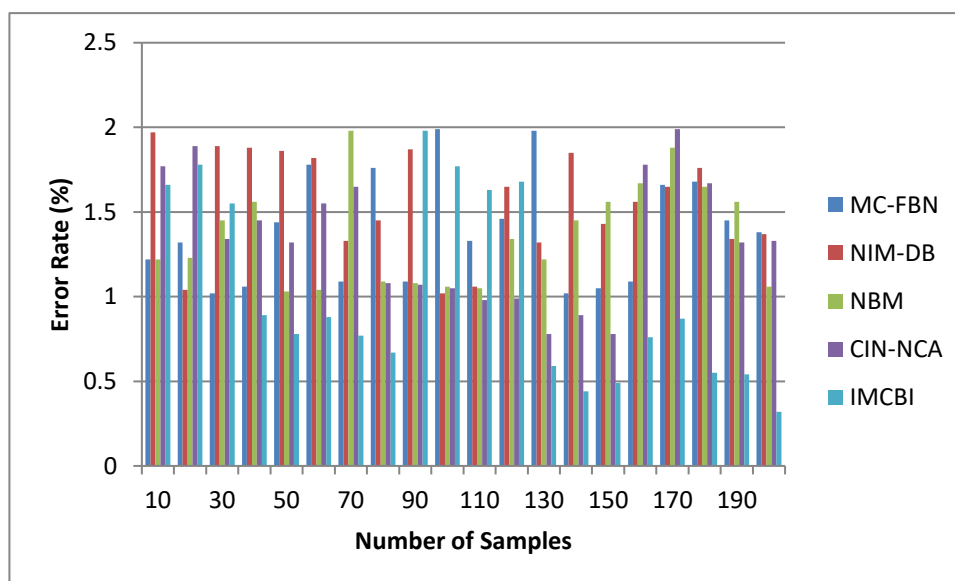


Figure 10: The error rate of the IMCBI method

The precision rate defined by Equation (21)

$$\text{Precision rate} = \frac{t_p}{t_p + f_p} \quad (21)$$

Both valid and incorrect positive numbers exist for the precision rate. The accuracy rate is just one element that affects how brain images are classified. Table 2 displays the accuracy and error rates of the IMCBI approach. It has been suggested to use the Improved Multi-Modal Cognitive Brain-Imaging Method (IMCBI) to detect brain activity resulting from various motor, perceptual, and cognitive tasks.

Table 2: IMCBI method with precision rate and error rate

Methods	Training set		Testing set	
	Precision rate	Error rate	Precision rate	Error rate
CIN-NCA	83.22	1.22	81.25	1.34
NBM	81.56	1.56	81.67	1.45
NIM-DB	82.78	1.89	82.98	1.33
MC-FBN	81.33	1.23	80.99	1.02
IMCBI	88.34	0.49	89.90	0.98

The multi-modal cognitive (MC) method has additional equivalent limitations $1 \leq r X_1$ for crucial instances and compared to standard ones. The functionality rate is represented as $\frac{B}{2} \sum_{r=1}^{R_1} \pi_r^2 + \sum_{r=R_1+1}^R \varepsilon_r \cdot \pi_r$. The optimization variable is unnecessary because interaction occurs by raising or reducing the gap is an equal chance. The correct variational procedure is represented by $b_r(v, a_r + d) \cdot c_r$. The variations are between the limitations for γ^r is the acceptable form of objective function according to the optimization techniques obtained by functionality rate. The functionality rate of the IMCBI is in figure 11.

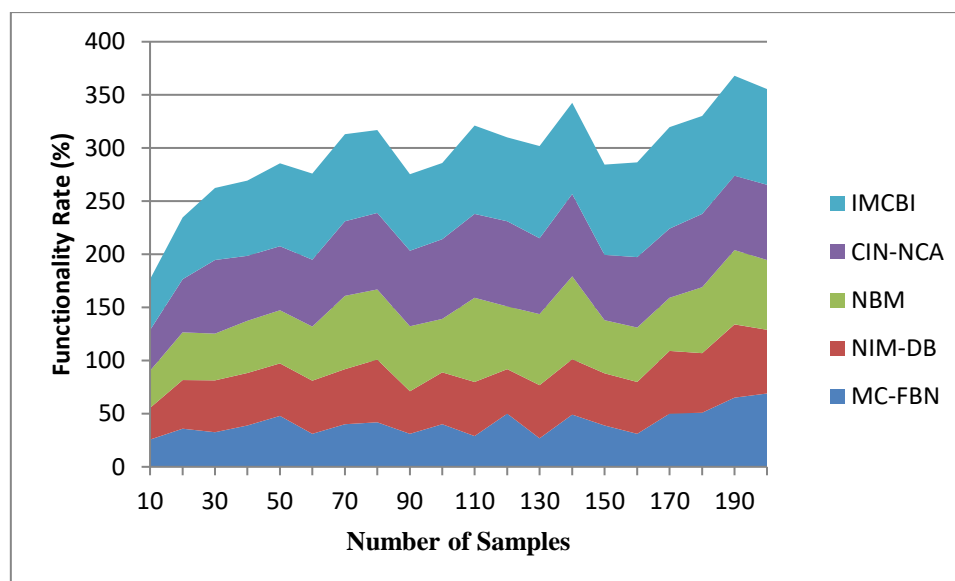


Figure 11: The functionality rate of the IMCBI method

Comparing the proposed IMCBI to other existing Multi-Region Correlation Based Functional Brain Network (MC-FBN), Non-cognitive Behavioral Model (NBM), Non-Invasive Imaging Modalities to Study Diseases of Aging Brain (NIM-DB), Cognitive Impairment and Network Connectivity Analysis, the proposed IMCBI attains the maximum classification accuracy, specificity, sensitivity, and precision rate (CIN-NCA).

5. Conclusion

This paper offerings the Improved Multi-modal cognitive brain-imaging method (IMCBI) to perceive brain activities from different motor, perceptual, and cognitive tasks. The human brain experiences imperative changes in its structural and functional architecture across its lifespan. However, traditional methods have several methodological challenges in identifying the brain region and classification based on insights into intelligent cognitive behavior for infants and adolescents. IMCBI is used for brain-imaging data to forecast a clinical or behavioral response. The use of mental success-dependent information for actual observations

strengthens the Multi-modal cognitive (MC) method training. The inter-subject retrieval method uses deep Neural Networks (DNN) to interpret behavioral activities in the human brain, which are collected from the functional magnetic resonance imaging (fMRI) data. The experiment's findings demonstrate that the proposed system is more accurate, sensitive, and specific in perceiving brain activity based on intelligent cognitive abilities than conventional counterparts, with accuracy ratios of 95.63%, 95.42%, and 94.33% when trained on images from Kaggle datasets.

Funding: "This research received no external funding"

Conflicts of Interest: "The authors declare no conflict of interest."

Reference

- [1] Mosconi L, Rahman A, Diaz I, Wu X, Scheyer O, Hristov HW, Vallabhajosula S, Isaacson RS, de Leon MJ, Brinton RD. Increased Alzheimer's risk during the menopause transition: A 3-year longitudinal brain imaging study. *PloS one*. 2018 Dec 12;13(12):e0207885.
- [2] Sen B, Borle NC, Greiner R, Brown MR. A general prediction model for the detection of ADHD and Autism using structural and functional MRI. *PloS one*. 2018 Apr 17;13(4):e0194856.
- [3] Bailey DM. Oxygen, evolution, and redox signaling in the human brain; quantum in the quotidian. *The Journal of physiology*. 2019 Jan;597(1):15-28.
- [4] Sarkar A, Harty S, Lehto SM, Moeller AH, Dinan TG, Dunbar RI, Cryan JF, Burnet PW. The microbiome in psychology and cognitive neuroscience. *Trends in cognitive sciences*. 2018 Jul 1;22(7):611-36.
- [5] Sleurs C, Blommaert J, Bataille D, Verly M, Sunaert S, Peeters R, Lemiere J, Uyttebroeck A, Deprez S. Cortical thinning and altered functional brain coherence in survivors of childhood sarcoma. *Brain imaging and behavior*. 2020 Apr 25.
- [6] Rahman, A.U., Saeed, M., Saeed, M.H., Zebari, D.A., Albahar, M., Abdulkareem, K.H., Al-Waisy, A.S. and Mohammed, M.A., 2023. A Framework for Susceptibility Analysis of Brain Tumours Based on Uncertain Analytical Cum Algorithmic Modeling. *Bioengineering*, 10(2), p.147.
- [7] De Luca R, Leonardi S, Portaro S, Le Cause M, De Domenico C, Colucci PV, Pranio F, Bramanti P, Calabrò RS. Innovative use of virtual reality in autism spectrum disorder: A case study. *Applied Neuropsychology: Child*. 2019 May 15:1-1.
- [8] Arahmane, H., Hamzaoui, E. M., Ben Maissa, Y., & Cherkaoui El Moursli, R. (2021). Neutron-gamma discrimination method based on blind source separation and machine learning. *Nuclear Science and Techniques*, 32(2), 18.
- [9] Devinsky O, Boesch JM, Cerda-Gonzalez S, Coffey B, Davis K, Friedman D, Hainline B, Houtp K, Lieberman D, Perry P, Prüss H. A cross-species approach to disorders affecting brain and behavior. *Nature Reviews Neurology*. 2018 Nov;14(11):677-86.
- [10] Devi SS, Singh NH, Laskar RH. Fuzzy C-Means Clustering with Histogram based Cluster Selection for Skin Lesion Segmentation using Non-Dermoscopic Images. *International Journal of Interactive Multimedia and Artificial Intelligence*. 2020;6(Special Issue on Soft Computing):26-31
- [11] Champagne-Jorgensen K, Kunze WA, Forsythe P, Bienenstock J, Neufeld KA. Antibiotics and the nervous system: More than just the microbes?. *Brain, Behavior, and Immunity*. 2019 Mar 1;77:7-15.
- [12] Gomathi, P., Baskar, S., Shakeel, P. M., & Dhulipala, V. S. (2020). Identifying brain abnormalities from electroencephalogram using evolutionary gravitational neocognitron neural network. *Multimedia Tools and Applications*, 79(15), 10609-10628. <https://doi.org/10.1007/s11042-019-7301-5>
- [13] Coenen A, Nelson JD, Gureckis TM. Asking the right questions about the psychology of human inquiry: Nine open challenges. *Psychonomic Bulletin & Review*. 2019 Oct 1;26(5):1548-87.
- [14] Rana Talib Rasheed, Mostafa Abdulgafoor Mohammed, & Nicolae Tapus. (2021). Big data analysis . *Mesopotamian Journal of Big Data*, 2021, 22–25. <https://doi.org/10.58496/MJBD/2021/004>
- [15] Torlasco C, Bilo G, Giuliano A, Soranna D, Ravaro S, Oliverio G, Faini A, Zambon A, Lombardi C, Parati G. Effects of acute exposure to moderate altitude on blood pressure and sleep breathing patterns. *International Journal of Cardiology*. 2020 Feb 15;301:173-9.
- [16] Hässler T, Shnabel N, Ullrich J, Arditti-Vogel A, SimanTov-Nachlieli I. Individual differences in system justification predict power and morality-related needs in advantaged and disadvantaged groups in response to group disparity. *Group Processes & Intergroup Relations*. 2019 Aug;22(5):746-66.
- [17] Worthman CM, Trang K. Dynamics of body time, social time, and life history at adolescence. *Nature*. 2018 Feb;554(7693):451-7.
- [18] Bebbington J, Unerman J. Achieving the United Nations sustainable development goals. *Accounting, Auditing & Accountability Journal*. 2018 Jan 15.
- [19] Zhu Q, Zhu J, Liu M, Xu X, Zhang D. Multi-Region Correlation Based Functional Brain Network for Disease Diagnosis and Cognitive States Detection. *IEEE Access*. 2018 Dec 4;6:78065-76.

- [20] Shulman RG, Rothman DL. A non-cognitive behavioral model for interpreting functional neuroimaging studies. *Frontiers in human neuroscience*. 2019 Mar 11;13:28.
- [21] Annavarapu RN, Kathi S, Vadla VK. Non-invasive imaging modalities to study neurodegenerative diseases of the aging brain. *Journal of chemical neuroanatomy*. 2019 Jan 1;95:54-69.
- [22] Wang Z, Zheng Y, Zhu DC, Bozoki AC, Li T. Classification of Alzheimer's disease, mild cognitive impairment, and stock control subjects using resting-state fMRI based network connectivity analysis. *IEEE journal of translational engineering in health and medicine*. 2018 Oct 15;6:1-9.
- [23] Ung WC, Yap KH, Ebenezer EG, Chin PS, Nordin N, Chan SC, Yip HL, Lu CK, Kiguchi M, Tang TB. Assessing Neural Compensation With Visuospatial Working Memory Load Using Near-Infrared Imaging. *IEEE Transactions on Neural Systems and Rehabilitation Engineering*. 2019 Nov 28;28(1):13-22.
- [24] Porras AR, Paniagua B, Ensel S, Keating R, Rogers GF, Enquobahrie A, Linguraru MG. Locally affine diffeomorphic surface registration and its application to surgical planning of frontal-orbital advancement. *IEEE transactions on medical imaging*. 2018 Mar 15;37(7):1690-700.
- [25] Hu W, Cai B, Zhang A, Calhoun VD, Wang YP. Deep collaborative learning with application to the study of multi-modal brain development. *IEEE Transactions on Biomedical Engineering*. 2019 Mar 13;66(12):3346-59.
- [26] <https://www.kaggle.com/tags/neuroscience>
- [27] Kurdi, S.Z., Ali, M.H., Jaber, M.M., Saba, T., Rehman, A. and Damaševičius, R., 2023. Brain Tumor Classification Using Meta-Heuristic Optimized Convolutional Neural Networks. *Journal of Personalized Medicine*, 13(2), p.181.
- [28] Ali, M.H., Jaber, M.M., Abd, S.K., Alkhayyat, A. and Jasim, A.D., 2022. Artificial Neural Network-Based Medical Diagnostics and Therapeutics. *International Journal of Pattern Recognition and Artificial Intelligence*.
- [29] Adnan, M.M., Rahim, M.S.M., Al-Jawaheri, K., Ali, M.H., Waheed, S.R. and Radie, A.H., 2020, September. A survey and analysis on image annotation. In 2020 3rd International Conference on Engineering Technology and its Applications (IICETA) (pp. 203-208). IEEE.